NRIAG JOURNAL OF ASTRONOMY AND GEOPHYSICS
2025, VOL. 14, NO. 1, 51–70
https://doi.org/10.1080/20909977.2025.2449791

Multi-technique subsoil characterisation in the coastal environment of Lekki Peninsula, Lagos, southwest Nigeria

Olawale Babatunde Olatinsu[a], Oluwafemi Adeyinka Adegbulugbe[a] and Amidu Abiola Ige-Adeyeye[a,b]

[a]Department of Physics, Faculty of Science, University of Lagos, Lagos, Nigeria; [b]Department of Physical Science, College of Basic Sciences, Lagos State University of Science and Technology, Ikorodu, Lagos, Nigeria

ABSTRACT

Integrated site investigations using VES techniques, SPT, borehole drilling, soil moisture content and specific gravity have been conducted at LFTZ, Lekki, Lagos, Nigeria. VES results correlated with borehole data revealed a lithological sequence with maximum five geoelectric layers. Inferred lithologies include low/moderate resistivity (45.6–206.3 Ωm) topsoil of sand/silty sand followed by a succession of silty sand/sand layers to a depth of about 45 m. Low depth silty sand (resistivity <300 Ωm) is the prevalent soil in the second and/or third strata and sand (resistivity >300 Ωm) is the last layer across the traverses. SPT results correlate well with borehole data showing a subsurface lithological sequence of very loose/loose grading silty sand, loose/medium dense grading silty sand, medium dense/dense grading sand and dense grading sand. Soil density Increases downward in boreholes with SPT N-values (2–24). Grain size distribution curves depict uniformly graded/narrowly graded soil aggregates with Cu and Cc in the ranges 1.33–8.00 and 0.610–2.00, respectively. Moderate moisture content values (16.72–27.82) suggest that the water table is close to the surface toward the nearby Atlantic Ocean. Specific gravity values (2.60–2.78) lie within the range for most soils and indicate that salinity is minimal at the study location.

ARTICLE HISTORY
Received 24 August 2024
Revised 1 December 2024
Accepted 1 January 2025

KEYWORDS
Geophysical technique; geotechnical investigation; geology; coastal environment; Lekki Peninsula, Nigeria

1. Introduction

In the last five decades, the impact of population growth on natural resources such as land, water, ecosystem services etc., has been overwhelming in virtually all major cities of the world (Cruz 1994; Garg 2017). Particularly, as the world's population continues to grow, there is a greater demand than ever for land development for continual human existence and sustainable development. Land reclamation in different geological terrains has increasingly been driven by the expanding need for residential, agricultural, industrial, commercial purposes and green space infrastructure, etc (McComas 1972; Sengupta et al. 2018; Zhang et al. 2021; Sheng et al. 2022). In Lagos Metropolis, the perennial population growth mainly due to rural–urban migration has prompted several developmental activities in pursuit of acquisition and expansion of land for human habitation. The civil engineering practice of coastal reclamation, which transforms coastal wetlands or shallow seas into dry land or enclosed shallow water bodies, is very popular in coastal communities. It entails a number of procedures, such as building a seawall, draining saltwater, and filling the enclosed area with different materials including rocks, gravel, and sand (Chapman 1984). The coastal areas of Lagos State such as Ikoyi, Lekki, Ajah etc. have been more impacted because they are attractive to settlements due to factors including economic opportunities, tourism, resources, and urbanisation trends. Land reclamation efforts and practices to resolve these existential conflicts between human needs and land resources have seen significant surges over time, posing enormous issues for coastal reclamation planning, sustainable growth, and coastal ecosystem conservation (Mostafa 2012; Burak and Kucukakca 2015; Gatto 2015; Olatinsu et al. 2019). Foundation and by extension, its peculiar ground environment, is a major factor that determines the longevity and ability of structures to cope with the stress of time, use, and some other inevitable natural situations. Within the Lagos metropolis, it is often common to find residential and commercial buildings and other infrastructure built on waste landfills and man-made fills, as well problematic soils rich in clay materials. Such ground conditions pose enormous structural stability issues which often result in fatal consequences to human lives and properties (Gidigasu 1972; Bain and Highley 1978; Oyelami and Van Rooy 2016; Agasnalli et al. 2022). Building in

CONTACT Olawale Babatunde Olatinsu oolatinsu@unilag.edu.ng Department of Physics, Faculty of Science, University of Lagos, Akoka Yaba, Lagos, Nigeria

coastal areas is notably challenging. Residential buildings and infrastructural facilities in coastal areas are particularly faced with challenges due to some natural occurrences such as breaking waves or strong wind, erosion and scour, high-velocity storm surge, moving floodwater, flood-borne debris etc. (Afolayan et al. 2014; Rahman and Rahman 2015; Owamah et al. 2018; Griggs and Reguero 2021; Hernández-Delgad 2024). With the intention of improving the state's economic standing, the Lagos State government created the Lekki Free Trade Zone in order to meet the increased demand for land, particularly on the Lekki Peninsula. This business concern is an offshoot of the 2006 Beijing Summit of the Forum on China-Africa Cooperation, and serves the construction of the Belt and Road Initiative. This special economic zone situated on a massive 16,500-hectare plot of land has been created to make the most of the strategic location of Lagos as a major West African distribution hub. A project of this magnitude is typically linked to significant infrastructure development, including high-rise buildings, bridges, and networks of roads and trains.

Except for cost implications, the importance of comprehensive site investigation embracing geological, geotechnical and geophysical techniques, in civil engineering projects cannot be overemphasised. This is due to the fact that it is a highly effective preliminary exercise that often uncovers critical subsoil conditions and features essential for foundation quality and bearing capacity of structures. The understanding of subsoil conditions is even more critical for foundations in very complex and highly inhomogeneous terrain such as coastal environments, for stability and durability of structures and their resilience to environmental stresses that might arise from the effects of climate change (Manap and Voulvoulis 2016; Boateng 2020; Ohenhen and Shirzaei 2022). Foundation in coastal areas must support the load of the building despite the forces of weathering and corrosion that are usually harsh. Unfavourable soil conditions may jeopardise a building's structural stability, perhaps leading to significant foundation damage and collapse. Remedying the damage may require expensive renovations.

Global statistics indicate that unanticipated ground conditions account for 80% of the construction project issues (Sanders 1994; Badu et al. 2013; Amarasekara et al. 2018; Loulakis and Gransberg 2022). Many buildings collapse has been reported in the Lagos metropolis and are more common in coastal areas (Oloke et al. 2017; Awoyera et al. 2021; Ohenhen and Shirzaei 2022; Alabi et al. 2023). These situations could have been prevented or handled more effectively had appropriate site characterisation procedures been conducted (Peacock 1990; Ashton and Gidado 2001). Weak or faulty foundations are the main factor responsible for the collapse of buildings and other infrastructure, and they are , typically, the direct consequence of building foundations on subsoil region with non-uniform composition, low strength and load bearing capacity. In addition, regions with these features are more likely to experience differential or unequal settling as a result of the supporting soil's inconsistent response.

Geotechnical analysis has been utilised to furnish relevant data relating to soil and rock conditions, groundwater levels, and possible risks that may have impart on the stability and safety of structures. Soil characterisation by sampling and in-situ testing such as standard penetration test (SPT), is a typical point-to-point investigation subject to some inevitable uncertainties such as measurement error, parameter uncertainty etc (Wagner 2020). However, interpretation of test results is not usually too complex because the relationship between the blow count (N-value) and the angle of shearing resistance is currently well established. Also, some regional and global relations between N-value and other soil engineering attributes are also known (Kulhawy and Mayne 1990). Hence, SPT is a straightforward and inexpensive process that is especially well-suited for cohesionless soils (Holtz and Kovacs 1981). Borehole drilling is also a point-to-point method of gaining more relevant data on the properties of the subsurface rock and soil (Kruse et al. 2018). By collecting samples and conducting numerous in-situ tests (such as moisture content and specific gravity), borehole investigations enable geotechnical engineers and other field specialists to better uncover the characteristics and locations of different soil/rock layers (Price 2009; Monnet 2015; Kruse et al. 2018). The positions of boreholes and their unique testing circumstances are key points in project's objectives (Kruse et al. 2018). In the absence of borehole data, the interpretation of geophysical and geotechnical data frequently introduces some degree of inconsistencies (Reynolds et al. 2017). For large-scale projects, drilling wells may be a cost intensive and intricate process requiring a lot of planning, equipment, and experience. The cost of drilling a borehole well depends on the well's depth, location, and geological circumstances (Danert et al. 2009).

However, the cost of the investigation can be significantly reduced by utilising geophysical survey in conjunction with geotechnical investigations (Azahar et al. 2019; Liu et al. 2023). This is due to the fact that geophysical techniques are extremely quick to implement, non-invasive and non-destructive, and can lower project duration (Sahoo et al. 2007; Preko et al. 2009; Capizzi et al. 2020). Geophysical techniques have been used in civil/geotechnical engineering projects for decades, from site characterisation to foundation quality assessment. Near surface site characterisation using seismic, electrical/electromagnetic and ground penetrating radar (GPR) methods often yields valuable information that relates to soil characteristics such as the spatial distribution of subsurface materials, elastic properties and electrical characteristics (Ward 1990; Reynolds 2011; Niederleithinger et al. 2012, 2015; Ikard et al. 2014, 2015; Rumpf and Tronicke 2014). These techniques have assisted greatly in improving structural imaging quality and spotting minute alterations in concretes. 1-D vertical electrical sounding (VES) surveys are widely utilised in geotechnical assessments for many applications in the building industry. VES techniques are a great reconnaissance tool to obtain a quick and accurate delineation of the electrical characteristics of soil/rock in various geological formations, which can help with foundation designs. This is because of their speedy, easy, and uncomplicated data gathering procedures. By gathering many 1-D soundings throughout an area, a 2-D pseudo-section of the subsurface resistivity distributions can be produced. Applications of VES in geotechnical works currently include groundwater exploration, where soil electrical resistivity can reveal groundwater accumulation; landfill mapping, since waste content affects soil electrical conductivity; earthing systems, in which it provides resistivity distribution profiles; pipeline route planning stages to facilitate the design and installations of buried pipelines since burial depth is a direct consequence of the external corrosion protection requirements; and soil lithology identifications, as variations in the electrical characteristics (resistivity or conductivity) of geological formations correspond to variations in their physical attributes. This study is a multi-technique approach aimed at detailed understanding of subsurface conditions at the Lekki Free Trade Zone, despite the presumed coastal geological complexity and heterogeneity. Data and the deductions from the integrated geological, geotechnical and geophysical investigations at this zone could serve as a guide in future foundation work and design that would engender stability and safety of structures and facilities.

2. Location and accessibility of the area

The study location is situated within the Lekki Free Trade Zone (LFTZ). LFTZ is a special economic zone designated within the Lekki Peninsula in the south-eastern axis of Lagos, southwest Nigeria. It is accessible through both sea and land. It shares boundary with the Atlantic Ocean towards the south (Figure 1) and the Lekki Lagoon towards the north. It is bordered by 5 km of coast line and stretches 50 km away from the centre of Lagos Metropolis. It is 70 km from the Murtala Mohammed International Airport (MMIA), 10 km from the site of the proposed Lekki international airport and 50 km from the Apapa Port, the largest port in West Africa. The LFTZ covers an expanse of land which is about 16,500 hectares and is linked through excellent road networks to the Lekki-Epe Expressway, a major transportation route in Lagos State. The strategic location of the LFTZ provides easy access to Lagos, Nigeria's commercial hub, and other major cities in the West African sub-region. Figure 2 shows a typical settlement within the study location close to the shore of the Atlantic Ocean.

3. The geology of the area

The geology of Nigeria is shared in almost equal proportions between the crystalline and sedimentary rocks (Burke et al. 1976; Woakes et al. 1987). The crystalline rocks consist of the Precambrian basement complex found mainly in parts of southwest and north central Nigeria (Figure 3). The Precambrian basement rocks comprise the Migmatite-Gneiss Complex, the Schist Belts (biotite, schist, quartzite schist and muscovite schists) and the Older Granites of the Early Proterozoic. The Younger granites which are predominantly magmatic rings of the Jurassic age are found mainly in Jos and parts of north-central Nigeria (Jones and Hockey 1964; Burke et al. 1976; Tijani 2023). The Sedimentary Basins (Figure 3), which include the Dahomey Basin, the Sokoto Basin, the Chad Basin, the Benue Trough, the Bida/Nupe Basin and the Niger Delta Basin are composed of sediment fill of the Cretaceous to Tertiary ages (Obaje 2009).

Some regions of southwest Nigeria fall within the Dahomey Basin in West Africa, which is a combination of inland/coastal/offshore basin that stretches from southeastern Ghana through Togo and the Republic of Benin to southwestern Nigeria to the Western margin of the Niger Delta Basin (Reyment 1965; Adegoke 1977). Lagos State lies on the eastern segment of the low-lying Dahomey Basin

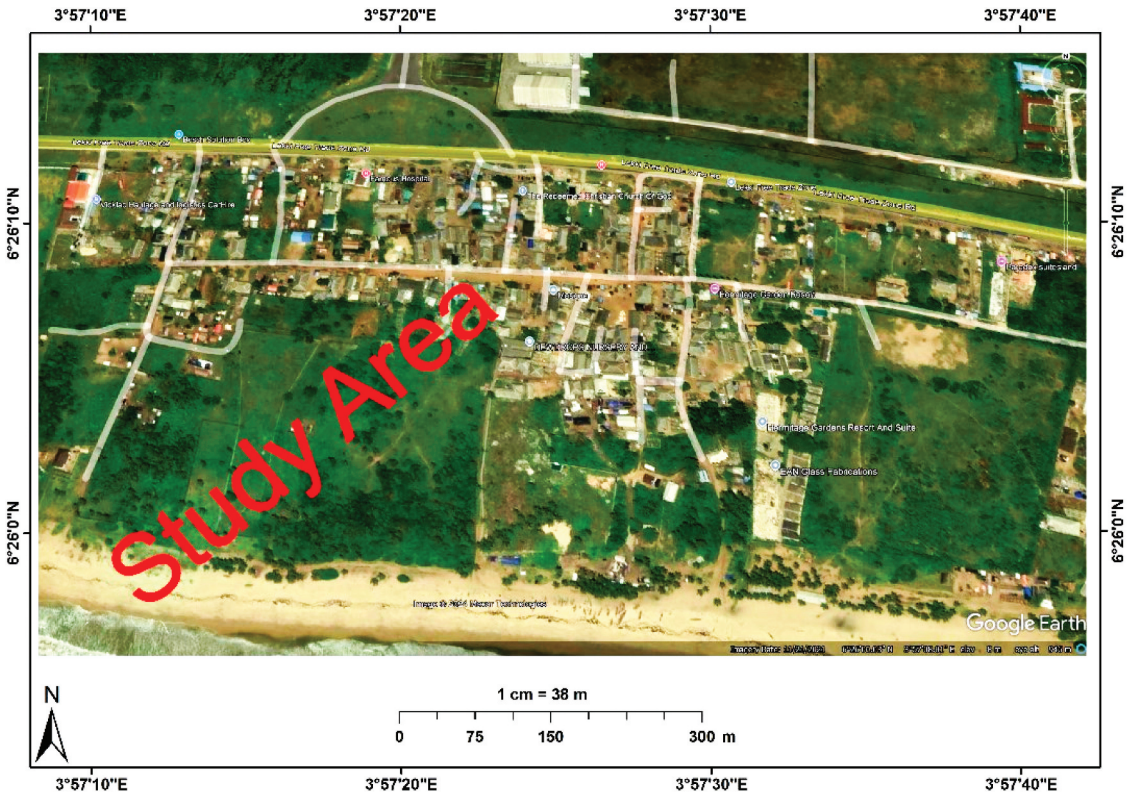

Figure 1. Google earth satellite image showing a 3D view of the study location and environs in Lekki, Lagos, Nigeria.

Figure 2. Some views of the settlements within the study location and environs close to the Atlantic Ocean in Lekki, Lagos, Nigeria.

in West Africa (Omatsola and Adegoke 1981). The base of the eastern Dahomey Basin consists of unfossiliferous sandstones and gravels obtained from the weathering of the underlying Precambrian basement. Overlying these are marine shales, sandstones and limestones from the Albian to Santonian ages deposited prior to the tectonic episode.

Lagos State is majorly littoral, low-lying and swampy, except for some areas inland. Several rivers in the southwest such as the Ogun, Osun, and, Yewa Rivers among others drain into the various Lagoons and creeks in Lagos such as the Lagos and Lekki lagoons, the Badagry creek etc (Awomeso et al. 2011). Lekki peninsula in Lagos State belongs to the coastal plain sand formation which is made up of loose sediment ranging from silt, clay and fine to coarse grained sand (Figure 3). The uncovered lithological unit in the area comprises of poorly sorted sediments of sands with lenses of clay (Adegoke et al. 1980; Longe et al. 1987). The sands are in part cross bedded and show transition to continental characteristics (Jones and Hockey 1964; Reyment 1965; Adegoke 1969).

4. Data acquisition and processing

The data acquisition map for the study depicted in Figure 4, shows the arrangement of the SPT points and VES stations along six traverses (TR1-TR6). For cross-

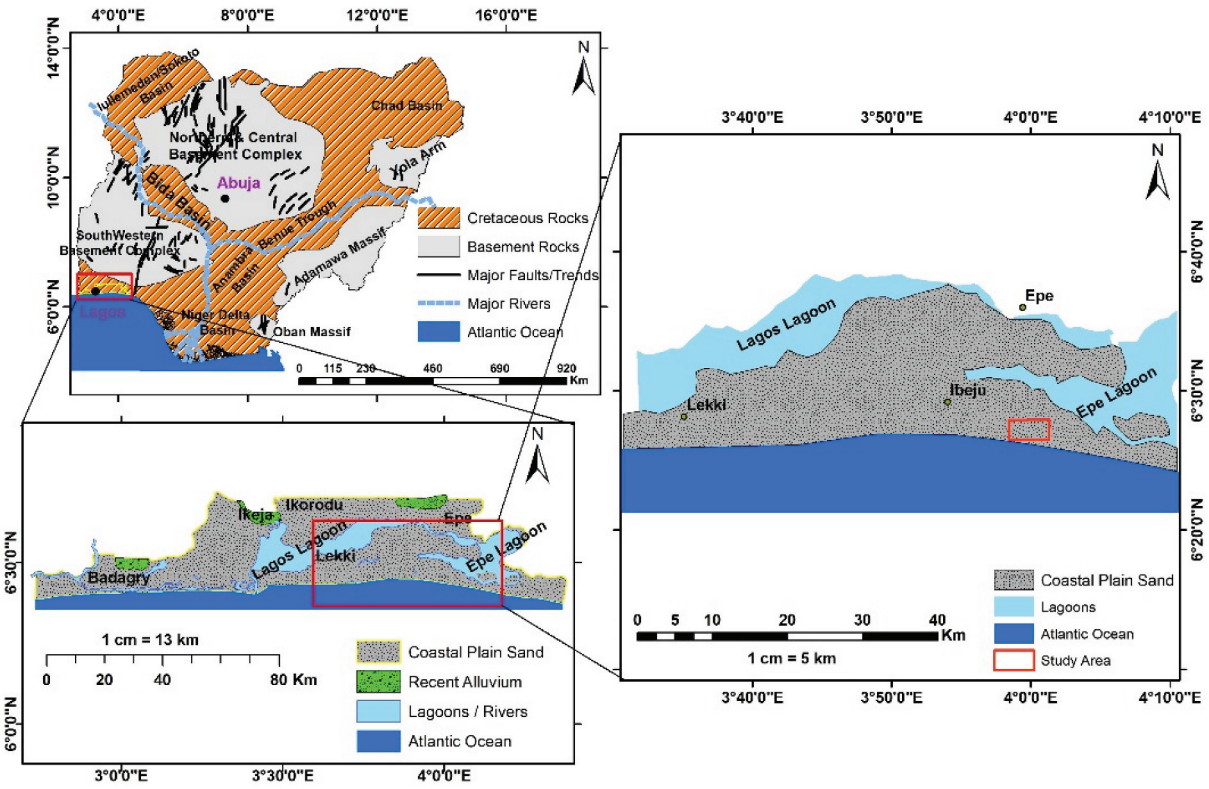

Figure 3. Geological map of Nigeria, Lagos State and Ibeju-Lekki. The study location the Lekki Free Trade Zone (LFTZ) within the Lekki peninsula falls within alluvial coastal deposit environment.

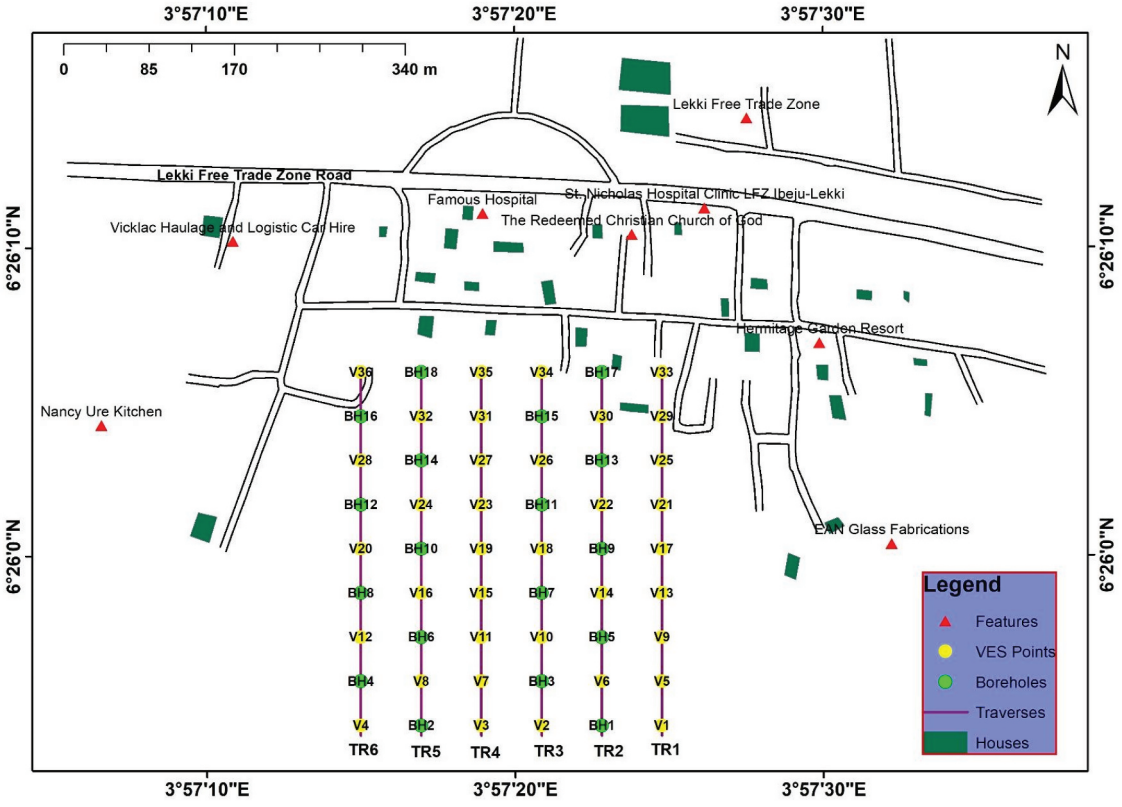

Figure 4. Data acquisition map showing the six traverses consisting of 36 resistivity sounding (VES) stations and 18 boreholes (BH) and other features around the study location.

correlation purpose so as to achieve a high level of confidence in the data analysis and interpretation, 36 VES stations and 18 SPT/borehole points were strategically distributed along the six equally spaced traverses to make up the grid-format field configuration (Figure 4). TR1 and TR4 each consist of nine VES stations only, TR2 and TR5 consist of five boreholes and four VES points, while TR3 and TR6 has four borehole and five VES points. Table 1 gives the coordinates (latitude and longitude) of all the boreholes and VES survey locations.

5. Electrical resistivity data

The VES technique permits fast data acquisition through discrete sampling of the subsurface at different depths along laid out profile lines (Ward 1990). VES data was acquired through the deployment of ABEM Terrameter SAS 1000 and its accessories. The surface position (x- and y-location) remains fixed, while the depth of the data point (z-position) varies during the survey. The Schlumberger configuration with four electrodes was employed, with two outer current electrodes

Table 1. Coordinates (latitude and longitude) of all the boreholes and VES survey locations.

Traverse	Borehole/VES	Latitude	Longitude
TR1	V1	6° 25′ 54.372″	3° 57′ 24.714″
	V5	6° 25′ 55.902″	3° 57′ 24.754″
	V9	6° 25′ 57.331″	3° 57′ 24.754″
	V13	6° 25′ 58.728″	3° 57′ 24.757″
	V17	6° 26′ 00.193″	3° 57′ 24.761″
	V21	6° 26′ 10.622″	3° 57′ 24.764″
	V25	6° 26′ 3.052″	3° 57′ 24.764″
	V29	6° 26′ 4.513″	3° 57′ 24.768″
	V33	6° 26′ 5.878″	3° 57′ 24.772″
TR2	BH1	6° 25′ 54.444″	3° 57′ 22.741″
	V6	6° 25′ 55.873″	3° 57′ 22.813″
	BH5	6° 25′ 57.403″	3° 57′ 22.817″
	V14	6° 25′ 58.696″	3° 57′ 22.817″
	BH9	6° 26′ 0.161″	3° 57′ 22.788″
	V22	6° 26′ 1.626″	3° 57′ 22.756″
	BH13	6° 26′ 3.124″	3° 57′ 22.792″
	V30	6° 26′ 4.452″	3° 57′ 22.795″
	BH17	6° 26′ 5.950″	3° 57′ 22.763″
TR3	V2	6° 25′ 54.412″	3° 57′ 20.837″
	BH3	6° 25′ 55.877″	3° 57′ 20.837″
	V10	6° 25′ 57.306″	3° 57′ 20.876″
	BH7	6° 25′ 58.735″	3° 57′ 20.844″
	V18	6° 26′ 0.164″	3° 57′ 20.848″
	BH11	6° 26′ 1.662″	3° 57′ 20.848″
	V26	6° 26′ 3.059″	3° 57′ 20.851″
	BH15	6° 26′ 4.520″	3° 57′ 20.855″
	V34	6° 26′ 5.885″	3° 57′ 20.858″
TR4	V3	6° 25′ 54.415″	3° 57′ 18.929″
	V7	6° 25′ 55.880″	3° 57′ 18.932″
	V11	6° 25′ 57.310″	3° 57′ 18.900″
	V15	6° 25′ 58.739″	3° 57′ 18.940″
	V19	6° 26′ 0.168″	3° 57′ 18.907″
	V23	6° 26′ 1.633″	3° 57′ 18.943″
	V27	6° 26′ 3.062″	3° 57′ 18.947″
	V31	6° 26′ 4.492″	3° 57′ 18.914″
	V35	6° 26′ 5.888″	3° 57′ 18.918″
TR5	BH1	6° 25′ 54.487″	3° 57′ 16.888″
	V6	6° 25′ 55.916″	3° 57′ 16.960″
	BH5	6° 25′ 57.346″	3° 57′ 16.895″
	V14	6° 25′ 58.742″	3° 57′ 16.895″
	BH9	6° 26′ 0.208″	3° 57′ 16.898″
	V22	6° 26′ 1.568″	3° 57′ 16.902″
	BH13	6° 26′ 3.066″	3° 57′ 16.906″
	V30	6° 26′ 4.427″	3° 57′ 16.906″
	BH17	6° 26′ 5.960″	3° 57′ 16.909″
TR6	V4	6° 25′ 54.491″	3° 57′ 14.947″
	BH4	6° 25′ 55.956″	3° 57′ 14.951″
	V12	6° 25′ 57.317″	3° 57′ 14.987″
	BH8	6° 25′ 58.714″	3° 57′ 14.958″
	V20	6° 26′ 0.211″	3° 57′ 14.994″
	BH12	6° 26′ 1.673″	3° 57′ 14.962″
	V28	6° 26′ 3.001″	3° 57′ 14.965″
	BH16	6° 26′ 4.499″	3° 57′ 15.001″
	V36	6° 26′ 5.928″	3° 57′ 14.969″

(A and B) assigned for injecting current and the other two inner potential electrodes (M and N) for measuring voltage (Telford et al. 1976; Dobrin and Savit 1988; Kearey et al. 2002; Lowrie and Fichtner 2020). The maximum current electrode spread (AB) and maximum potential electrode separation (MN) were 400 m and 14 m, respectively. The measuring system/equipment measures the apparent resistivity from a specific "focus" point which has specific x-, y- and z-coordinates. Thus, the apparent resistivity was determined at increasing depths by gradually extending the distance between the current electrodes while maintaining the centre of the four-electrode array unchanged.

Data processing was implemented with the use of WinGLinK software (SLB Inc.) for the initial filtering of data and visualisation. Apparent resistivity obtained by multiplying the point-by-point resistance with the corresponding geometric factor was plotted against half current electrode spacing. The filtered data were then imported into the WinResist software (Vander Velpen 2004) for fast computer data iteration to obtain final layer resistivities and thicknesses. Samples of the resistivity curves from the WinResist software exported into the MATLAB 2020a programming software are presented in Figure 5. The summary of results from VES interpretation (layer resistivities and thicknesses) was used to generate the geoelectric cross-sections at each VES location with the aid of ArcGIS software (ESRI Inc.) based on correlation with borehole data collected near the respective sounding stations.

6. SPT and borehole data

Standard Penetration Test (SPT) as an in-situ dynamic testing procedure is useful for the determination and evaluation of geotechnical engineering properties of subsurface soils at project sites (Parry 1978; Rogers 2009; Selvam et al. 2020). The relative densities of soils and the estimated shear strength parameters can be determined with this easy and affordable test. The SPT surveys is a repetitive procedure, which involves three operations: drilling the hole, penetration testing and sampling. This test was carried out with Shell and Auger borehole drilling method at 18 locations arranged along four traverses TR2, TR3, TR5 and TR6 (Figure 4). Borehole data through collection of soil samples was also obtained simultaneously along with SPT investigation at desired sampling depth depending on the borehole environments. The N-values were recorded for every 1.5 m depth intervals to a depth of about 30 m. The soil type of different colour and grade were classified as either silty sand or sand. The interpreted results from SPT procedure are usually used to estimate the geotechnical engineering properties of soil and for correlation with the electrical resistivity variations of the various encountered lithologies.

7. Grain size, moisture content and specific gravity data

7.1. Grain size analysis

Reports that are now available indicate that in areas with stable temperatures, the distribution of particle sizes significantly influences the other geotechnical properties of soil (Gidigasu 1972). Therefore, an attempt was made to identify and classify subsoils at the study location via grain size analysis. Grain size analysis was conducted on the samples collected the borehole drilling process SPT investigation. Grain size distribution curves were obtained from the standard sieve analysis of samples. The soil samples were shaken through a series of sieves with progressively smaller apertures. Before the soil sample is put through the

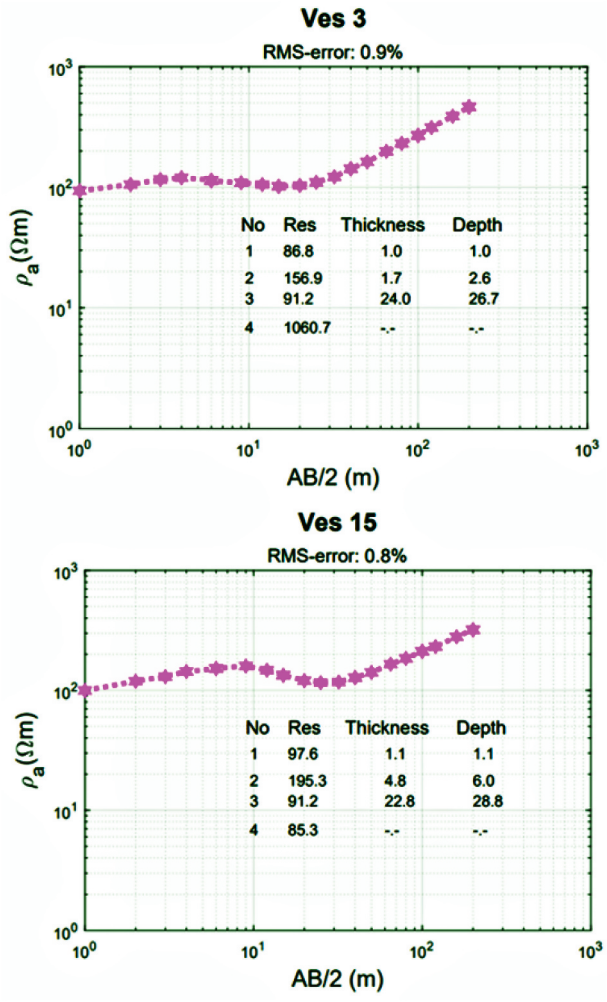

Figure 5. Samples of resistivity curve obtained after data processing.

sieves, it is first dried in an oven with any lumps of soil broken up into little pieces. The soil sample was then fed through the stacked sieve "tower" in order to conduct the test, which involved piling a sequence of sieves with progressively smaller mesh sizes on top of one another. Consequently, the soil particles are distributed as they are retained by the different sieves. Additionally, a pan was utilised to gather the particles that made it through the last sieve. The sizes of the opening used are 4.75, 2.36, 1.18, 0.60, 0.425, 0.3, 0.212, 0.15 and 0.075 mm. Based on the range of the particle sizes (particle size distribution), soils can be classified in the generic categories such as clay, silt, sand (fine, medium, dense) and gravel (ASTM 2006; AASHTO 2012). Further categorisations are also possible based on the analysis of the grain size distribution curves (Carter and Bentley 2016). The cumulative weight percentage of passing grain is plotted against the mesh size of the sieves, D, determined from the distribution curves (Figure 6). The coefficient of uniformity, C_u, is the ratio of D_{60} to D_{10} as given in Equation (1), where D_{60} and D_{10} are the mesh sizes from which 60% and 10% (Hazen's effective size) of the grains have passed, respectively (Bell 2007, 2016). The coefficient of gradation or curvature, C_c, is calculated using Equation (2), where D_{30} is the mesh size in which 30% of the grain have passed (Bell 2013).

$$C_u = \frac{D_{60}}{D_{10}} \tag{1}$$

$$Cc = \frac{D^2{}_{30}}{D_{60} \times D_{10}} \tag{2}$$

7.2. Moisture content

The moisture content (water content) of soil is an indicator of the amount of water present in soil. It is the ratio of the mass of water contained in the pore spaces of soil to the solid mass of particles in that material, expressed as a percentage (Carter and Bentley 2016; ASTM 2019). The standard temperature of 110 ± 5°C was used to determine the mass of the sample. Soil moisture was removed by oven-drying the soil samples until the weight remains constant. The moisture content in percent (%) was computed using the values of the weight of the sample recorded before and after drying, respectively.

7.3. Specific gravity

The specific gravity of soils and rocks is a significant property in geomechanics and geotechnics (Federico et al. 2018). Specific gravity can be used to determine the proportion of different minerals in a soil sample and to classify soils for engineering purposes. However, specific gravity alone is not enough to classify a soil, it is used in conjunction with other soil properties such as texture, consistency and mineralogy to classify a soil (Federico et al. 2018). The pycnometer technique was used for the estimation of the specific gravity of the collected soil samples. Known volume of dry soil samples were placed into the empty pycnometer, and then distilled water was added to fill the container. After removing all entrapped air bubbles, the pycnometer was weighed, and the weight of the sample and liquid together was determined. The process was then repeated with only the distilled water to obtain a reference weight, allowing for the calculation of the soil's specific gravity values.

8. Results and discussion

8.1. Geoelectric cross-sections and boreholes

Geoelectric cross-sections (Figures 7–12) were created using ArcGIS software (ESRI Inc.) to show the lithologies that were inferred from the VES results through

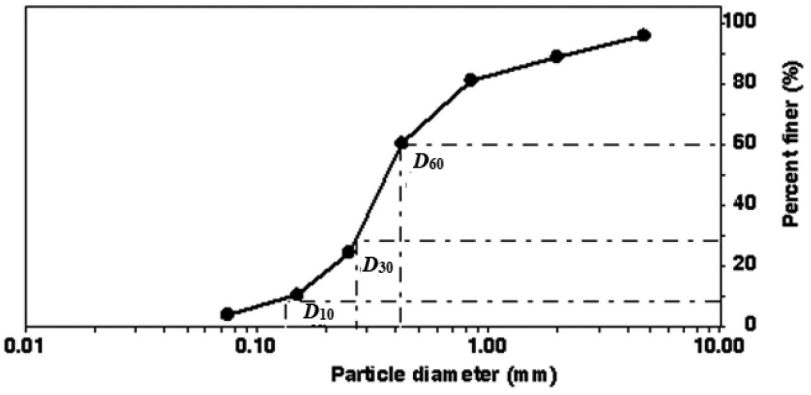

Figure 6. Grain-size distribution curve showing D_{10}, D_{30}, and D_{60} finer points respectively.

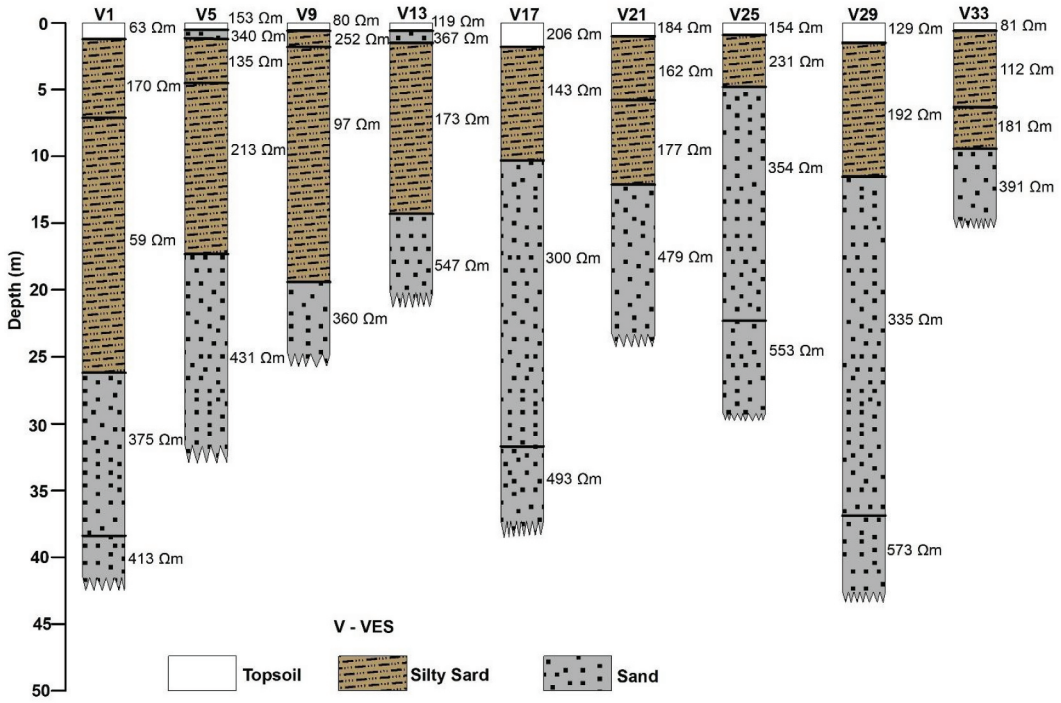

Figure 7. Geoelectric cross-sections obtained beneath TR1 comprising of only nine resistivity sounding stations – VES1, 5, 9, 13, 17, 21, 25, 29 and 33.

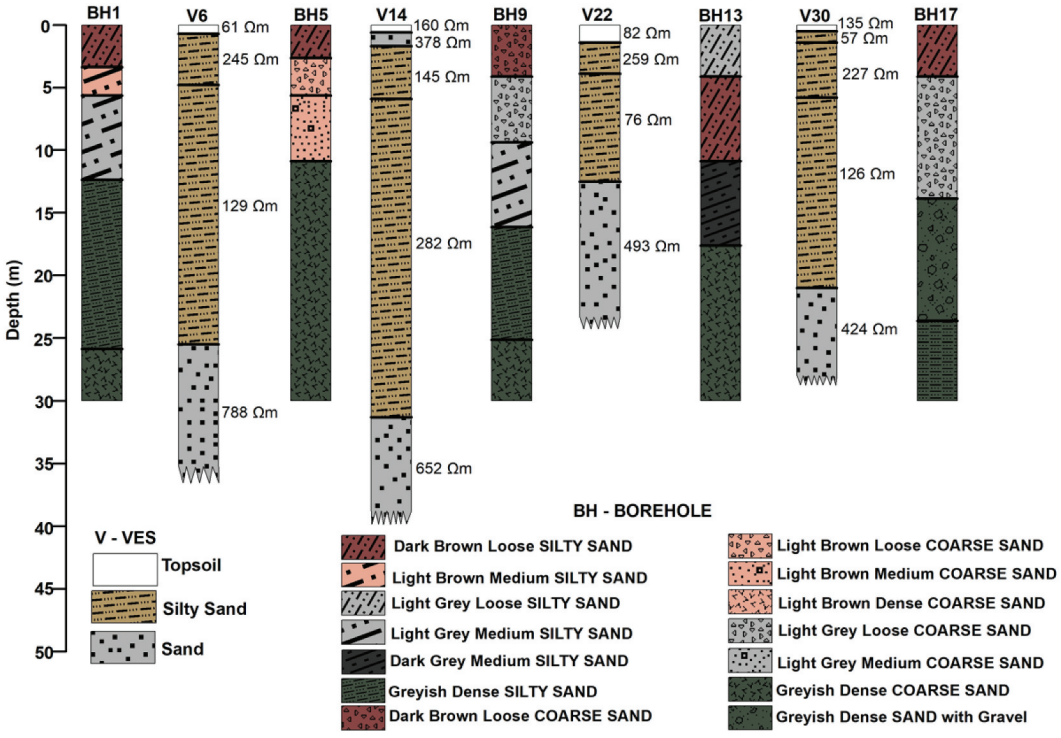

Figure 8. Geologic cross-section obtained for TR2 comprising of four resistivity sounding stations VES8, 16, 24, 32 and boreholes BH2, 6, 10, 14, 18.

correlation with borehole data. These cross-sections depict a less complex lithological succession with some geoelectric layers occurring more than once. The geoelectric section reveals a minimum of four geoelectrical layers (VES2, 3, 6–9, 11, 13, 15–17, 21–26, 28, 29, 31, 35, and 36) and a maximum of five geoelectrical layers (VES1, 4, 5, 10, 12, 14, 18–20, 27, 30, 32, and 34). At each of the 36 surveyed points, the layers sequence

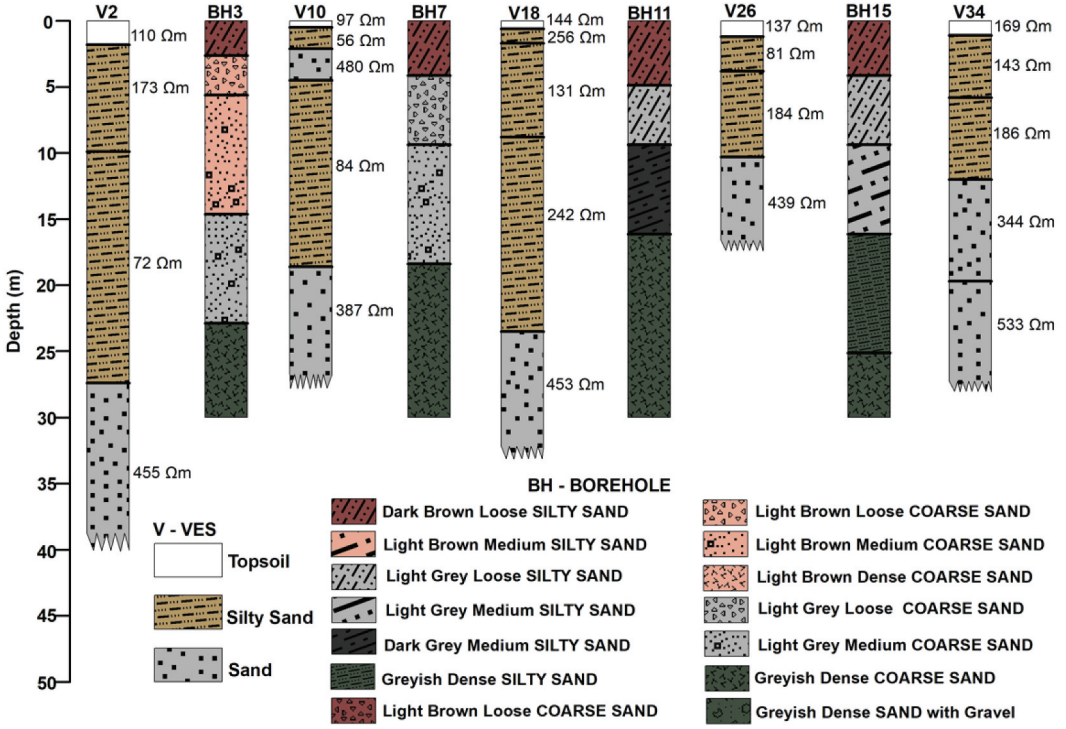

Figure 9. Geologic cross-section along TR3 comprising of four resistivity sounding stations VES8, 16, 24, 32 and boreholes BH2, 6, 10, 14, 18.

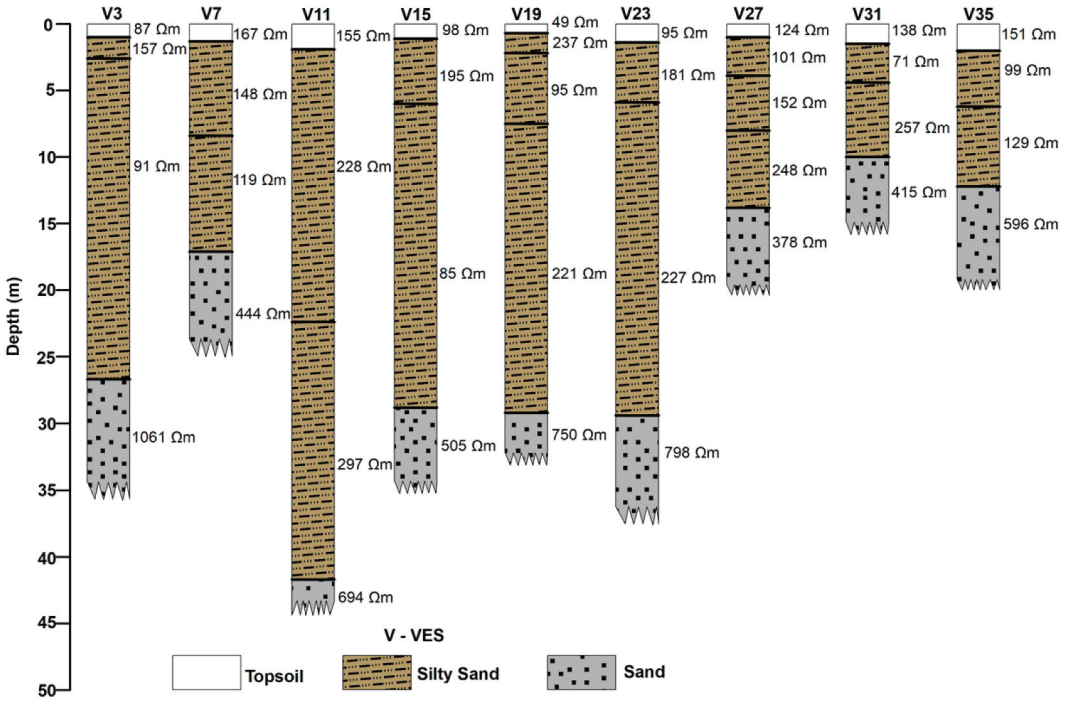

Figure 10. Geoelectric cross-sections obtained beneath TR4 comprising of only nine resistivity sounding stations – VES3, 7, 11, 15, 19, 23, 27, 31 and 35.

consisting of topsoil, more than one silty sand and/or sand layers are identified. The topsoil, which constitutes the first layer across all the six traverses, is primarily made up of sand or silty sand mixed with organic matter and detritus, as evident in the low to medium resistivity values. The ranges of the topsoil resistivity and thickness are 45.6–206.3 Ωm and 0.4–2.0 m, respectively. Nearly all the VES stations have second and/or third layers

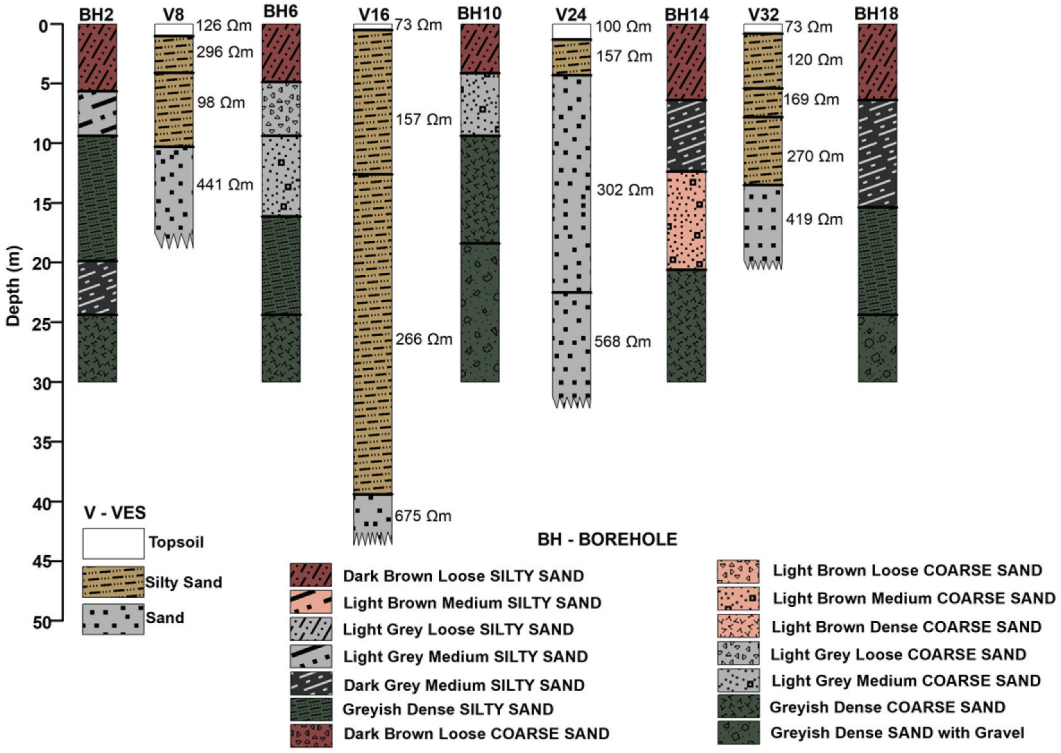

Figure 11. Geologic cross-section along TR5 comprising of four resistivity sounding stations VES8, 16, 24, 32 and boreholes BH2, 6, 10, 14, 18.

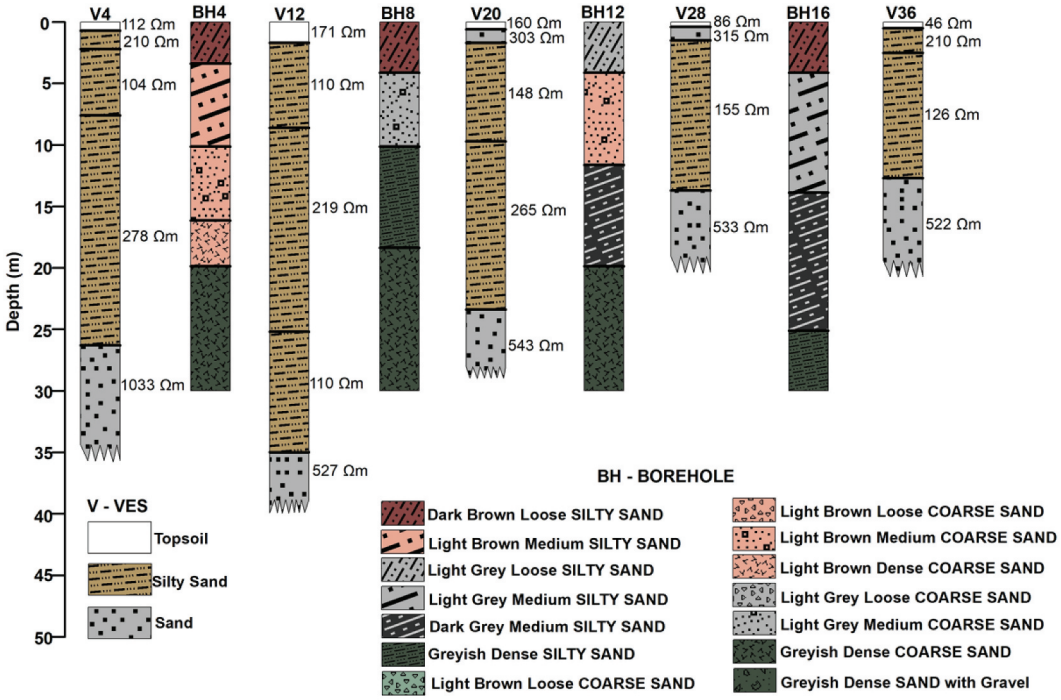

Figure 12. Geologic cross-section along TR6 comprising of five resistivity sounding stations VES4, 12, 20, 28, 36 and 4 boreholes BH4, 8, 12, 16.

Table 2. Resistivity values assigned to lithologies.

S/N	Resistivity (Ωm)	Lithology
1	46–206	Topsoil (Silty sand/sand mixed with organic matter/debris)
2	<300	Silty sand
3	>300	Sand

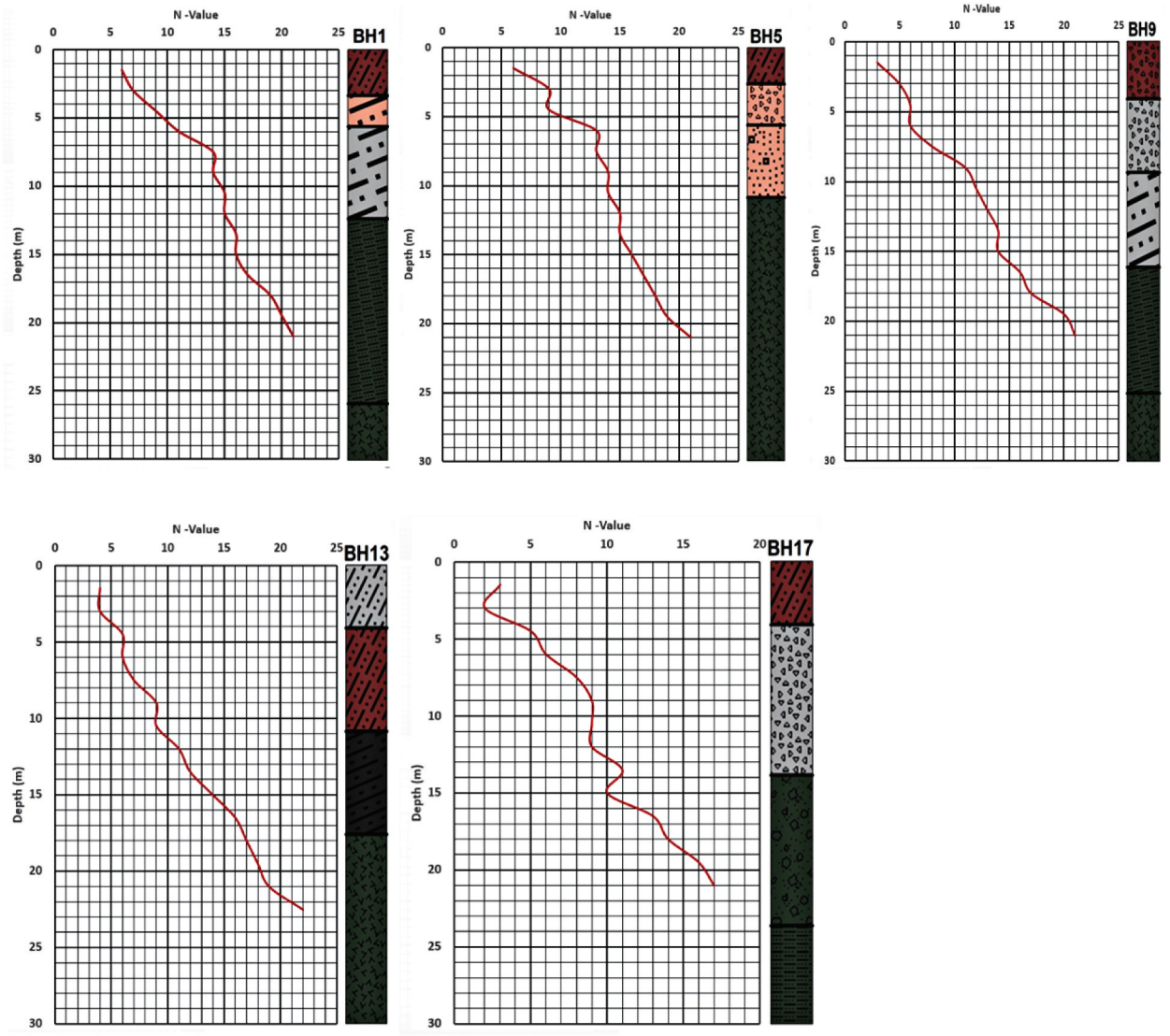

Figure 13. Correlation of borehole data with SPT curve along TR2.

containing silty sand with resistivity less than 300 Ωm (Table 2) and depths ranging from 7.1 to 41.7 m. The sand medium with resistivity greater than 300 Ωm was encountered as the last layer in virtually across the traverses.

8.2. SPT and borehole interpretation

The extracted data from samples taken at depths from the boreholes shows fair correlation with the SPT N-values, which range from a minimum of 2 to a maximum of 24, thus exhibiting a distinct increasing trend as depth increases. The variations in the subsurface conditions observed in borehole data could be due to the fact that some parts of the location were reclaimed by dredging of sand bodies from the nearby Atlantic Ocean. The SPT profiles for the 18 boreholes (Figures 13–16) clearly demonstrate an increase in density from the top of the boreholes to the base. The intercalations of layers of very loose or loose grading silty sand, loose to medium dense grading silty sand, medium dense to dense grading sand, and dense grading sand are the main sequence from the top of boreholes to the base. Furthermore, low grade unconsolidated topsoil and silty sand are typically associated with low N-values between 2 and 7, whereas more compact and competent sand subsoil encountered deeper into the subsurface strata is associated with comparatively high SPT-N values between 10 and 24.

8.3. Grain size, moisture content and specific gravity interpretation

Samples of the grain size distribution curves obtained by plotting the respective particle sizes against the percent finer are shown in Figure 17.

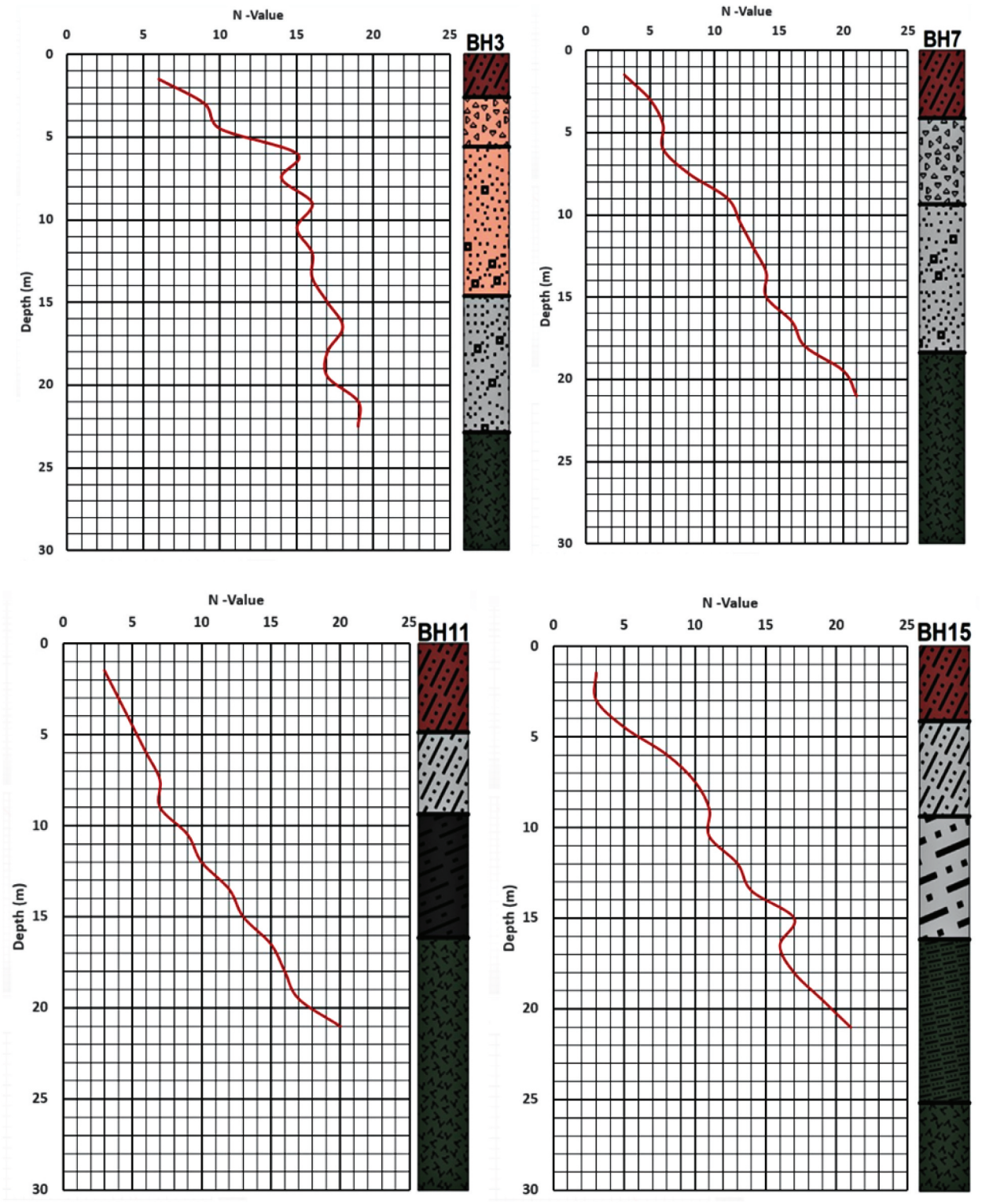

Figure 14. Correlation of borehole data with SPT curve along TR3.

The observed trend of these curves indicates that a high percentage of the particles in the soil aggregates have sizes that fall within specific ranges, indicating that the soils are either uniformly graded or narrowly graded. Table 3 displays the calculated values of the uniformity coefficient C_u and the coefficient of gradation C_c from Equations (1) and (2). Classification of soil quality is based on the values of C_u and C_c. If C_u is more than 6 and C_c is between 1 and 3, sand is said to be well

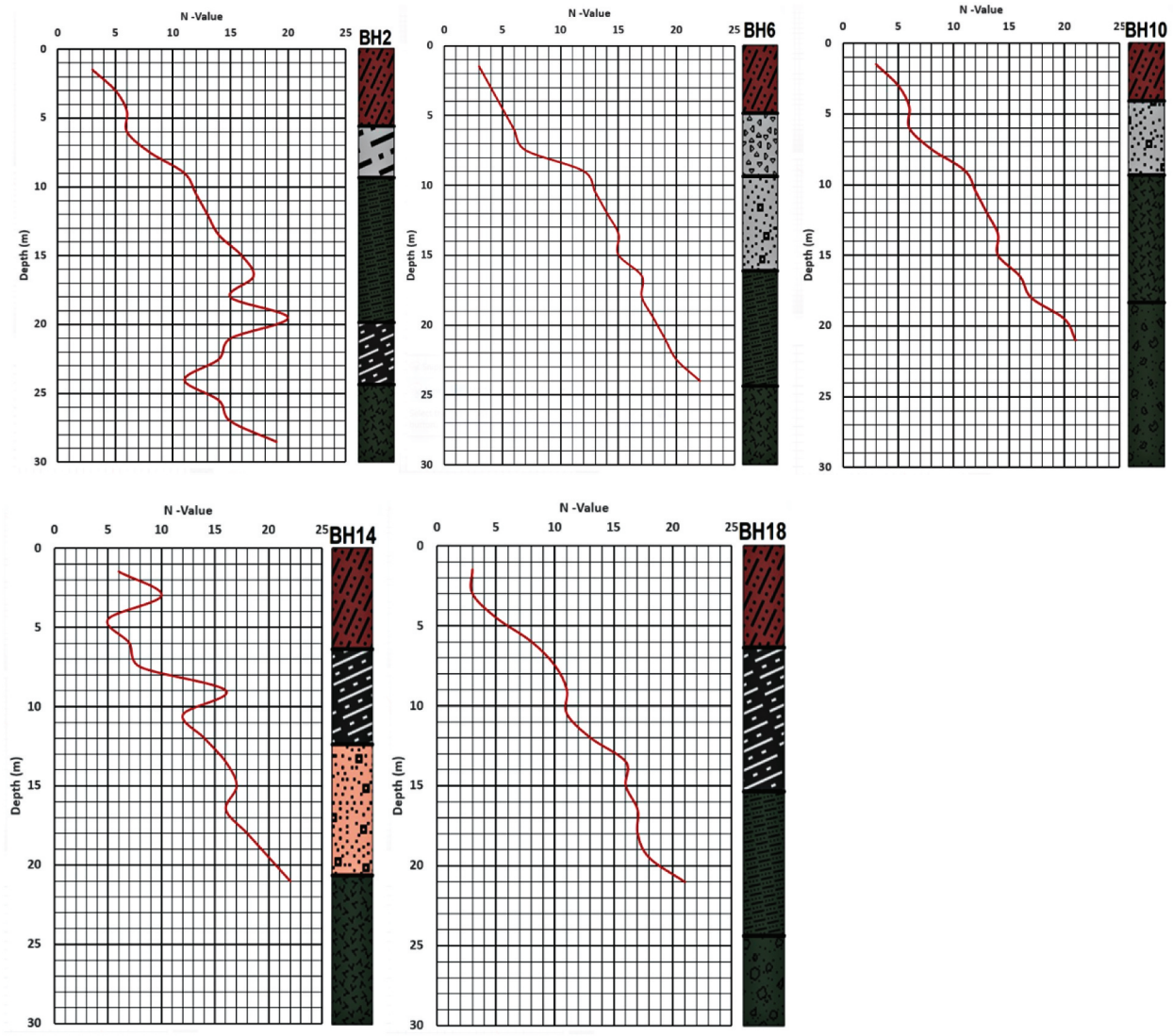

Figure 15. Correlation of borehole data with SPT curve along TR5.

graded. C_u must be higher than 4 and C_c must be between 1 and 3 for gravel to be deemed properly graded. The calculated C_u and C_c values for the collected samples at different depths lie within the ranges 1.33–8.00 and 0.61–2.00 respectively. According to the Unified Soil Classification System, these values imply that the soil samples at the study location up to the investigated depth are mostly sandy and generally not well graded. They contain poorly graded sand grains with very few fine grains as observed on the distribution curves. The only exception is in BH2 at a depth of 7.50 m which has computed values C_u and C_c as 8.00 and 2.00, respectively.

The moisture content of the soil samples collected from the drilled borehole increases fairly with depth (Table 3). These moderate values suggest that the water table in the area is close to the surface and can be linked to the proximity of the study location to the Atlantic Ocean and that the soils are moderately saturated and porous. Soil moisture content directly affects compaction conditions. Insufficient compaction due to improper moisture levels can result in unstable foundations and compromised structural integrity. The values of the specific gravity of the studied soils range from 2.60 to 2.78 and for most soils, the values are usually within the range 2.65–2.80. This shows that the effect of salinity is very minimal. Rahil et al. (2019) reported a decrease in the specific gravity values of clayey soils from three different locations in the Baghdad area at a depth about 1.5 m below natural ground surface, as the salt content increases. This decrement was attributed to the low specific gravity values of sodium salt (NaCl). Although specific gravity is not a direct

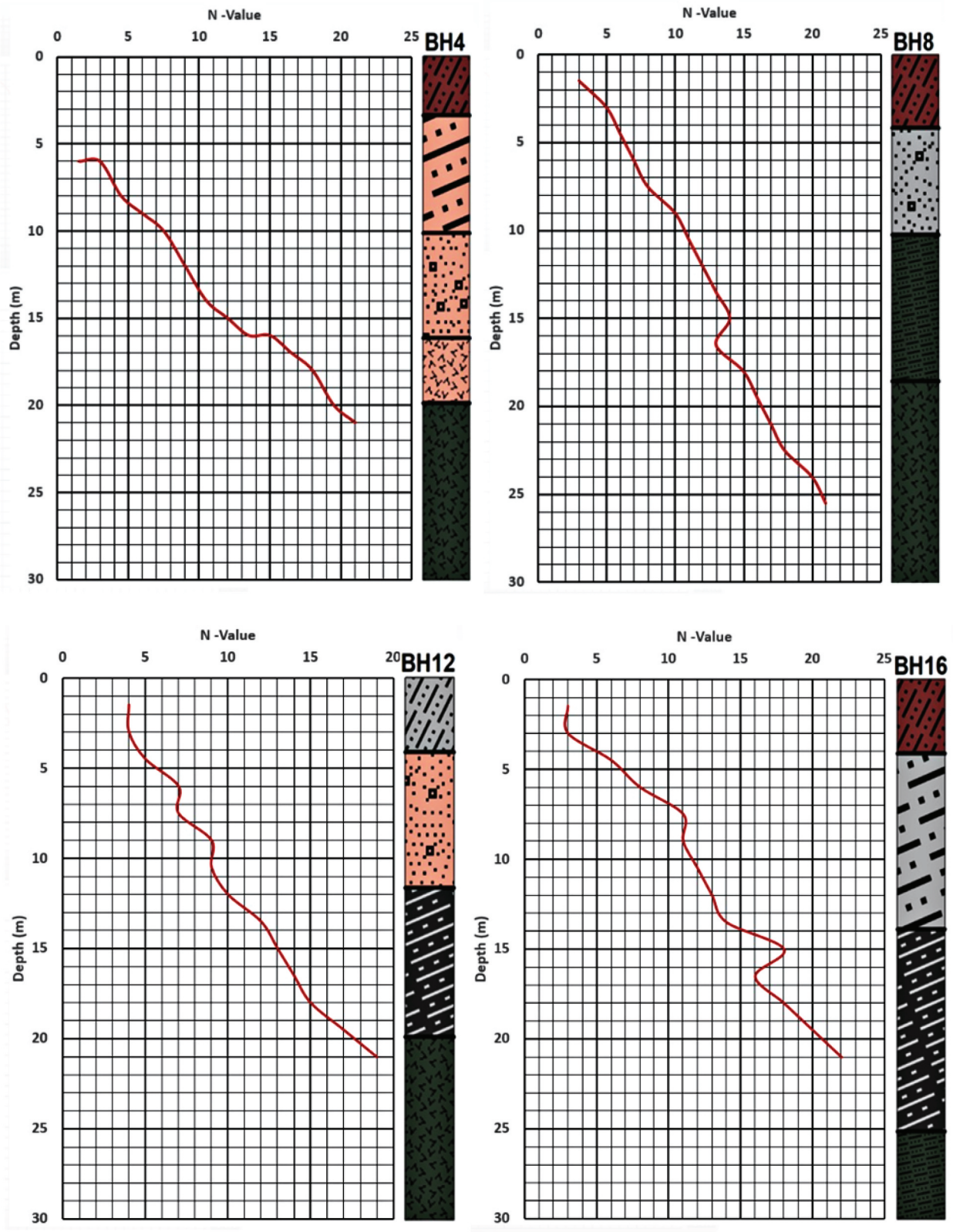

Figure 16. Correlation of borehole data with SPT curve along TR6.

measure of a soil's strength, it is a significant physical characteristic that can reveal vital information about the characteristics and contents of a soil that ultimately influence strength. Construction and geotechnical engineers can use their knowledge of the link between specific gravity and other soil properties to design and construct structures above or within soil.

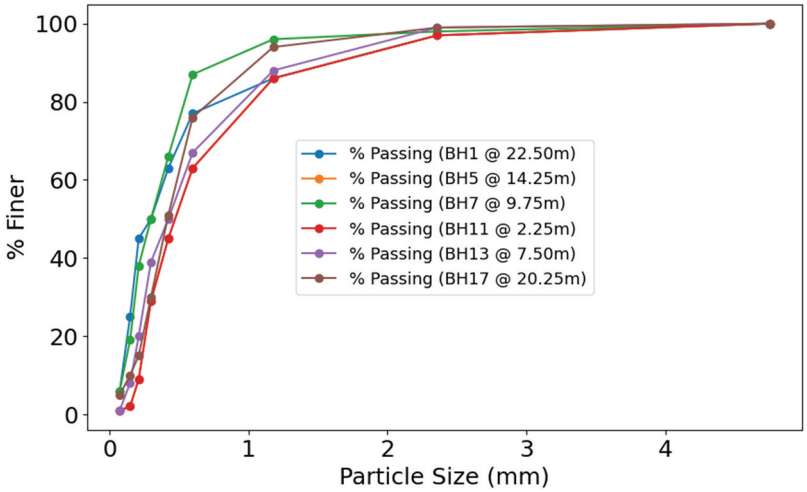

Figure 17. Some selected samples of the grain size distribution curves obtained by plotting the percent finer with the corresponding sieve sizes. Pattern of these curves typify soil aggregates with high proportion of the particles having sizes with narrow limits i.e. uniform soils or narrowly graded soils.

9. Conclusion

The integration of multiple subsoil characterisation techniques viz: SPT, electrical resistivity, borehole drilling, soil moisture content and specific gravity at Lekki Free Trade Zone, in Lekki Peninsula, Lagos peninsula has provided comprehensive data on the subsoil conditions vital for pre-construction consideration. Interpreted vertical electrical sounding data correlated with the borehole data revealed a less complex lithological sequence of a maximum of five geoelectric layers. The topsoil is composed of a mixture of sand/silty sand and organic matter/plant debris. as evident in the low to medium resistivity values 45.6–206.3 Ωm at a maximum depth of 2.0 m. A succession of silty sand and sand layers of diverse grading underlie the topsoil to a depth of about 45 m. Silty sand with resistivity less than 300 Ωm was delineated as the prevalent soil type in the second and/or third strata at low depth except at few locations where it occurred at greater depth. The sand layers with resistivity greater than 300 Ωm was encountered as the last layer in virtually all the traverses..

SPT curves depict increasing soil density from the top of the boreholes to the base in agreement with increasing SPT N-values with depth. This observed trend actually represent a subsurface arrangement consisting of very loose/loose grading silty sand, loose/medium dense grading silty sand, medium dense/dense grading sand and dense grading sand as inferred from the boreholes. Low SPT N-values (2–7) are connected with low grade unconsolidated topsoil/silty sand, while the relatively higher SPT N-values (10–24) correlate with the denser and more competent sand layers. Computed C_u (1.33–8.00) and C_c (0.610–2.00) values from grain size analysis are signatures of soil samples that are majorly sandy and generally poorly graded. These values also reveal the soils are permeable and fairly saturated. Moisture content and specific gravity values of the analysed soil samples attest to the proximity of the study location to the Atlantic Ocean.

Observed trend of grain size distribution curves indicate that a higher percentage of certain soil aggregates which are either uniformly graded or narrowly graded. The calculated C_u and C_c values computed for the samples at the different depths lie within the ranges 1.33–8.00 and 0.61–2.00, respectively. These values reveal that the soil samples up to the investigated depth are mostly poorly graded sand grains with very few fine grains. The only exception is at BH2 where C_u (8.00) and C_c (2.00) are quite higher at depth 7.50 m.

The moderate moisture content values of the soil samples (16.72–27.82) increase fairly with depth, which suggest that the water table in the study area is at shallow depth and is most likely associated with nearness to the Atlantic Ocean. Additionally, this also implies increasing soil compaction down the boreholes. The specific gravity values of the studied soils range from 2.60 to 2.78. This lie within the within the range of 2.65–2.80 for most soils. Hence, salinity, which tends to decrease the specific gravity of soils, has negligible effect on subsoils at the study location. However, construction professionals need to rely on available data on other soil properties to ascertain soil strength at the location for proper design of foundations. Finally, comprehensive site investigation using appropriate geophysical subsurface method in conjunction with geotechnical and geological subsoil characterisation is necessary in coastal locations, especially where land reclamation

Table 3. Summary of borehole lithology encountered with moisture content and specific gravity and computations from grain size analyses.

Borehole	Surface elevation (m)	Sampled depth (m)	Moisture content	Specific gravity	Uniformity coefficient C_u	Coefficient of gradation C_c	Lithology encountered
BH1	−2.00	0.75	17.21	2.60	2.22	0.61	Silty sand
		6.00	19.20	2.64	2.00	0.72	Silty sand
		12.75	22.10	2.70	2.22	0.61	Silty sand
		22.50	25.20	2.78	4.00	0.90	Sand
BH2	−2.75	1.50	17.25	2.63	4.40	0.90	Silty sand
		7.50	19.32	2.67	8.00	2.00	Sand
		16.50	21.70	2.69	3.80	1.05	Silty sand
		26.25	25.60	2.71	4.00	1.00	Sand
BH3	−3.00	4.50	18.89	2.65	4.00	0.81	Sand
		9.00	19.45	2.68	4.00	1.00	Sand
		18.75	22.10	2.72	4.44	0.91	Sand
		30.00			4.00	0.81	Sand
BH4	−2.80	2.25	17.42	2.62	2.20	1.64	Silty sand
		10.50	20.59	2.69	2.67	0.67	Sand
		15.75	23.70	2.72	2.00	0.72	Sand
		29.25	27.82	2.75	3.00	1.20	Sand
BH5	−2.90	0.25	17.21	2.61	2.10	1.02	Silty sand
		9.75	19.50	2.68	2.11	0.59	Sand
		14.25	22.25	2.71	3.00	0.75	Sand
		23.25	24.70	2.75	4.00	1.00	Sand
BH6	−2.00	3.00	18.71	2.63	3.80	0.85	Silty sand
		8.25	19.52	2.67	3.50	1.14	Sand
		19.50	24.00	2.72	4.00	1.00	Silty sand
		21.75	25.10	2.71	4.00	1.00	Sand
BH7	−0.1	5.25	18.90	2.64	3.33	1.48	Sand
		9.75	19.62	2.68	4.00	1.00	Sand
		17.25	24.20	2.71	2.20	1.64	Sand
		24.75	26.50	2.72	2.67	0.67	Sand
BH8	−0.30	3.75	18.79	2.63	2.22	0.56	Silty sand
		6.75	19.05	2.66	2.67	0.67	Sand
		18.00	24.20	2.72	2.67	0.67	Silty sand
		24.00	25.72	2.76	2.67	0.67	Sand
BH9	−0.10	1.50	18.20	2.64	2.22	0.56	Sand
		11.25	21.21	2.70	3.80	1.05	Silty sand
		15.00	22.50	2.69	3.00	0.75	Silty sand
		27.00	26.50	2.78	4.00	1.00	Sand
BH10	−0.30	0.75	18.21	2.62	2.33	0.53	Silty sand
		12.00	22.01	2.70	2.67	0.67	Sand
		20.25	24.82	2.74	3.00	1.33	Sand
		24.75	26.67	2.75	3.33	1.48	Sand
BH11	−1.70	2.25	18.51	2.60	2.00	1.13	Silty sand
		8.25	19.54	2.71	3.80	1.05	Silty sand
		13.50	22.31	2.65	4.30	0.93	Silty sand
		25.50	25.40	2.74	2.22	0.56	Sand
BH12	−1.50	3.00	18.52	2.67	2.40	0.74	Silty sand
		6.00	18.82	2.64	4.08	1.00	Silty sand
		14.25	22.00	2.72	2.15	1.05	Silty sand
		27.75	26.40	2.74	2.22	0.80	Sand
BH13	−1.80	4.50	18.97	2.59	3.00	1.20	Silty sand
		7.50	19.29	2.65	2.78	0.54	Silty sand
		18.00	24.43	2.70	3.33	0.92	Sand
		28.50	26.21	2.73	3.00	1.33	Sand
BH14	−2.00m	0.25	16.92	2.63	2.10	1.07	Silty sand
		9.00	19.48	2.69	2.90	1.38	Silty sand
		18.75	22.91	2.73	3.90	1.03	Sand
		21.00	23.67	2.71	5.00	0.80	Sand
BH15	−0.90	5.25	19.00	2.64	2.53	0.70	Silty sand
		10.50	20.70	2.67	3.33	0.53	Silty sand
		15.75	23.52	2.73	1.33	0.96	Silty sand
		22.50	25.18	2.72	2.53	0.70	Silty sand
BH16	−1.00	6.75	19.46	2.63	2.53	0.70	Silty sand
		12.00	22.01	2.69	2.53	0.70	Silty sand
		19.50	24.00	2.73	2.53	0.70	Silty sand
		30.00	26.90	2.78	2.53	0.70	Silty sand
BH17	−2.00	0.75	16.72	2.61	2.67	0.54	Silty sand
		11.25	20.42	2.59	2.22	0.67	Sand & gravel
		20.25	24.00	2.71	2.93	1.36	Sand & gravel
		29.25	27.21	2.75	4.00	1.00	Silty sand
BH18	−1.50	0.75	17.02	2.58	2.22	0.67	Silty sand
		8.25	19.43	2.63	3.80	1.05	Silty sand
		15.00	23.51	2.74	2.11	0.59	Silty sand
		25.50	26.23	2.70	2.53	0.70	Silty sand & gravel

through soil dredging has been widely deployed. This would certainly assist in preventing the emergence of unstable foundations that are inimical to the integrity of structures.

Acknowledgments

The authors wish to thank Mr. Anuoluwapo Oladipupo of Lagos State Material Testing Laboratory for his assistance in getting some data for the research.

Disclosure statement

No potential conflict of interest was reported by the author(s).

ORCID

Olawale Babatunde Olatinsu http://orcid.org/0000-0002-0412-1972

References

AASHTO. 2012. Classification of soils and soil-aggregate mixtures for highway construction purposes. M145-91. (WA) (DC), USA: American Association of State Highway and Transportation Officials.

Adegoke OS. 1969. Eocene Stratigraphy of Southern Nigeria. Collogue sur Eocene Vol. III. Bur. Rech. Geol. Min. Mem 69. 23–48.

Adegoke OS. 1977. Stratigraphy and paleontology of the ewekoro formation (Paleocene) of South Western Nigeria. Bull Paleont. 71(295), 299-316.

Adegoke OS, Jeje LK, Durotoye B, Adeleye DR, Ebukanson EJ. 1980. The geomorphology and aspects of sedimentology of coastal region of Western Nigeria. J Min Geol. 7(2):217–223.

Afolayan AD, Olumayowa AA, Oyeronke AO. 2014. Geotechnical properties of selected beach sands in Lagos, Southwestern Nigeria. Geosciences. 4(3):51–53. doi: 10.5923/j.geo.20140403.01.

Agasnalli C, Deepak MS, Reddy CNA. 2022. Global view of lateritic soil improvement for construction purposes in tropical countries. Mater Today: Proc. 65(2):1895–1899. doi: 10.1016/j.matpr.2022.05.158.

Alabi OM, Mustaffa NE, Aminuddin FA. 2023. A review on error-induced-building collapse at the construction stage in Lagos, Nigeria. IOP Conf Ser: Earth Environ Sci. 1274 (1):012026. doi: 10.1088/1755-1315/1274/1/012026.

Amarasekara WDL, Perera BAKS, Rodrigo MNN. 2018. Impact of differing site conditions on construction projects. J Legal Aff Dispute Resolut Eng Construct. 10 (3):04518006. doi: 10.1061/(ASCE)LA.1943-4170.0000257.

Ashton P, Gidado K. 2001. Risk associated with inadequate site investigation procedures under design and build procurement systems. In: Akintoye A editor. 17th Annual ARCOM Conference, 5-7 September 2001, University of Salford, Association of Researchers in Construction Management, Vol. 1. p. 961–969.

ASTM. 2006. Standard practice for classification of soils for engineering purposes (Unified soil classification system). West Conshohocken (PA), USA; p. D2487.

ASTM. 2019. Standard test methods for laboratory determination of water (moisture) content of soil and rock by mass. ASTM International, D2216 – 19. 7pp.

Awomeso JA, Taiwo AM, Morawo OA, Moyosore JO. 2011. Possible abstraction sites along Osun River lower course in Ogun and Lagos States, Nigeria for sustainable supply of potable water. J Sci Technol. 31(3):58–67. doi: 10.4314/just.v31i3.7.

Awoyera PO, Alfa J, Odetoyan A, Akinwumi II. 2021. Building collapse in Nigeria during recent years: causes, effects, and way forward. IOP Conf Ser: Mater Sci Eng. 1036(1):012021. doi: 10.1088/1757-899x/1036/1/012021.

Azahar MA, Mahadi NFZ, Rusli QN, Narendranathan N, Lee EC. 2019. Use of geophysics for site investigations and earthworks assessments. IOP Conference Series: Materials Science and Engineering, 512:012007. doi: 10.1088/1757-899x/512/1/012007.

Badu E, Owusu-Manu D, Edwards JD, Adesi M, Lichtenstein S. 2013. Rural infrastructure development in the Volta region of Ghana: barriers and interventions. J Financ Manage Property Constr. 18 (2):142–159. doi: 10.1108/JFMPC-11-2012-0040.

Bain JA, Highley DE. 1978. Regional appraisal of clay resources. A challenge to the clay mineralogist. Proceedings of the IV International Clay Conference AIPEA; [1978 July 10–14]; Oxford; 437–458.

Bell FG. 2007. Engineering geology. 2nd ed. Oxford: Butterworth Heinemann.

Bell FG. 2013. Engineering properties of soils and rocks. Amsterdam: Elsevier.

Bell FG. 2016. Fundamentals of engineering geology. Amsterdam: Elsevier.

Boateng FG. 2020. Building collapse in cities in Ghana: a case for a historical institutional grounding for building risks in developing countries. Int J Disaster Risk Reduct. 50:101912. doi: 10.1016/j.ijdrr.2020.101912.

Burak S, Kucukakca E. 2015. Impact of land reclamation on the coastal areas in Istanbul. Geophysical research abstracts, EGU2015-4881, EGU General Assembly 2015, 12-17 April, 2015, Vienna, Austria. id.4881, vol 17.

Burke K, Freeth SJ, Grant NK. 1976. The structure and sequence of geological events in the basement complex of the Ibadan area, Western Nigeria. Precambrian Res. 3 (6):537–545. doi: 10.1016/0301-9268(76)90017-6.

Capizzi P, Martorana R, Pirrera C, Ventura Bordenca G, Saggio C. 2020. Application of non-invasive seismic techniques for the characterisation of a gravity concrete dam. Explor Geophys. 52(3):1–14. doi: 10.1080/08123985.2020.1823210.

Carter M, Bentley SP. 2016. Soil properties and their correlations. 2nd ed. New Jersey (USA): John Wiley & Sons, Ltd. Hoboken.

Chapman DM 1984. The edge of the sea. In: Schwartz M, editor. Beaches and coastal Geology. Springer US.

Cruz MCJ. 1994. Population pressure and land degradation in developing countries. In: Population, environment and development. (NY): United Nations; p. 135–147.

Danert K, Carter RC, Adekile D, MacDonald A. 2009. Cost-effective boreholes in sub-Saharan Africa. Guidelines for community supply and protection in africa. NERC Open Research Archive. https://nora.nerc.ac.uk.

Dobrin MB, Savit CH. 1988. Introduction to geophysical prospecting. New York (USA): McGraw-Hill Publishing Company.

Federico AM, Miccoli D, Murianni A, Vitone C. 2018. An indirect determination of the specific gravity of soil

solids. Eng Geol. 239:22–26. doi: 10.1016/j.enggeo.2018.03.013.
Garg S. 2017. Impact of overpopulation on land use pattern. In: Environmental issues surrounding human overpopulation. USA: IGI Global; p. 137–154.
Gatto M. 2015. Does reclamation pay? Assessing the socio-economic effects of reclamation projects. Terra Et Aqua. (38):25–35.
Gidigasu MD. 1972. Mode of formation and geotechnical characteristics of laterite materials of Ghana in relation to soil forming factors. Eng Geol. 6(2):79–150. doi: 10.1016/0013-7952(72)90034-8.
Griggs G, Reguero BG. 2021. Coastal adaptation to climate change and sea-level rise. Water. 13(16):2151. doi: 10.3390/w13162151.
Hernández-Delgad EA. 2024. Coastal restoration challenges and strategies for small island developing states in the face of sea level rise and climate change. Coasts. 4 (2):235–286. doi: 10.3390/coasts4020014.
Holtz RD, Kovacs WD. 1981. An introduction to geotechnical engineering. (NJ): Prentice-Hall.
Ikard SJ, Revil A, Schmutz M, Karaoulis M, Jardani A, Mooney MA. 2014. Characterization of focused seepage through an earthfill dam using geoelectric methods. Groundwater. 52(6):952–965. doi: 10.1111/gwat.12151.
Ikard SJ, Rittgers J, Revil A, Mooney MA. 2015. Geophysical investigation of seepage beneath an earthen dam. Groundwater. 53(2):238–250. doi: 10.1111/gwat.12185.
Jones HA, Hockey RD. 1964. The geology of part of south western Nigeria. Geol Survey Nigeria, Bull. 31:1–101.
Kearey P, Hill I, Brooks M. 2002. An introduction to geophysical exploration. 3rd ed. Hoboken (NJ), USA: Wiley-Blackwell. ISBN: 978-0-632-04929-5.
Kruse E, Eslamian S, Ostad-Ali-Askari K, Hosseini-Teshnizi SZ. 2018. Borehole investigations. In: Bobrowsky PT Marker B, editors. Encyclopedia of engineering geology. Springer International Publishing AG. doi: 10.1007/978-3-319-12127-7_32-2.
Kulhawy FH, Mayne PW. 1990. Manual on estimating soil properties for foundation design. Electric Power Research Institute EL-6800, project 1493-6. Palo Alto (CA), USA: Electric Power Research Institute.
Liu Y, Ng YCH, Zhang Y, Yang P, Ku T. 2023. Incorporating geotechnical and geophysical investigations for underground obstruction detection: a case study. Undergr Space. 11:116–129. doi: 10.1016/j.undsp.2022.12.003.
Longe EO, Malomo S, Olorunniwo MA. 1987. Hydrogeology of Lagos metropolis. J Afr Earth Sci (1983). 6(2):163–174. doi: 10.1016/0899-5362(87)90058-3.
Loulakis MC, Gransberg DD. 2022. Managing the risk of subsurface conditions. NAC Executive Insights, National Academy of Construction, EI 6.4.
Lowrie W, Fichtner A. 2020. Fundamentals of geophysics. 3rd ed. Cambridge, (UK): Cambridge University Press. doi: 10.1017/9781108685917.
Manap N, Voulvoulis N. 2016. Data analysis for environmental impact of dredging. J Cleaner Prod. 137:394–404.
McComas MR. 1972. Geology and land reclamation. Ohio J Sci. 72(2):65–75.
Monnet J. 2015. In situ tests in geotechnical engineering 398. (NY): Wiley.
Mostafa Y. 2012. Environmental impacts of dredging and land reclamation at Abu Qir Bay, Egypt. Ain Shams Eng J. 3(1):1–15. doi: 10.1016/j.asej.2011.12.004.
Niederleithinger E, Abraham O, Mooney M. 2015. Geophysical methods in civil engineering: overview and new concepts. International Symposium Non-Destructive Testing in Civil Engineering (NDT-CE); [2015 Sep 15–17]; Berlin, Germany.
Niederleithinger E, Weller A, Lewis R. 2012. Evaluation of geophysical techniques for dike inspection. J Environ Eng Geophys. 17(4):185–195. doi: 10.2113/JEEG17.4.185.
Obaje NG. 2009. The basement complex. In: Geology and mineral resources of Nigeria. Lecture notes in earth sciences Vol. 120, Berlin, Heidelberg: Springer. doi: 10.1007/978-3-540-92685-6_2.
Ohenhen LO, Shirzaei M. 2022. Land subsidence hazard and building collapse risk in the coastal city of Lagos, West Africa. Earth's Future. 10(12):e2022EF003219. doi: 10.1029/2022EF003219.
Olatinsu OB, Oyedele KF, Ige-Adeyeye AA. 2019. Electrical resistivity mapping as a tool for post-reclamation assessment of subsurface condition at a sand-filled site in Lagos, southwest Nigeria. SN Appl Sci. 1(24). doi: 10.1007/s42452-018-0028-5.
Oloke OC, Oni AS, Ogunde A, Opeyemi J, Babalola DO. 2017. Incessant building collapse in Nigeria: a framework for post-development management control. Dev Ctry Stud. 7(3):114–127.
Omatsola ME, Adegoke OS. 1981. Tectonic evolution and cretaceous stratigraphy of Dahomey Basin. J Mineral Geol. 18:130–137.
Owamah HI, Ukala DC, Apkan E, Ukala DC. 2018. Assessment of some geotechnical properties of Nigerian coastal soil: a case-study of Port-Harcourt beach mud. J Appl Sci Environ Manag. 22(2):228. doi: 10.4314/jasem.v22i2.13.
Oyelami CA, Van Rooy JL. 2016. A review of the use of lateritic soils in the construction/development of sustainable housing in Africa: a geological perspective. J Afr Earth Sci. 119:226–237. doi: 10.1016/j.jafrearsci.2016.03.018.
Parry RH. 1978. Estimating bearing capacity of sand from SPT values. J Geotech Eng Div ASCE. 103(9):1014–1019. doi: 10.1061/AJGEB6.0000484.
Peacock WS. 1990. Site investigation procedures and risk analysis. University of Manchester, UMIST [PhD thesis]. Dept. of Civil and Structural Eng. Institute of Science and Technology.
Preko K, Scheuermann A, Wilhelm H. 2009. Comparison of invasive and non-invasive electromagnetic methods in soil water content estimation of a dike model. J Geophys Eng. 6(2):146–161. doi: 10.1088/1742-2132/6/2/006.
Price DG. 2009. Engineering geology: principles and practice. In: De Freitas MH, editors. 450. Berlin: Springer. ISBN 3-540-29249-7.
Rahil FH, Al-Soudany KYH, Abbas NS, Hussein LY. 2019. Geotechnical properties of clayey soils induced by the presence of sodium chloride. IOP Conference Series: Materials Science and Engineering, 518:022064. doi:10.1088/1757-899x/518/2/022064.
Rahman S, Rahman MA. 2015. Climate extremes and challenges to infrastructure development in coastal cities in Bangladesh. Weather Clim Extremes. 7:96–108. doi: 10.1016/j.wace.2014.07.004.
Reyment RA. 1965. Aspects of the geology of Nigeria: the stratigraphy of the cretaceous and Cenozoic deposits Ibadan University Press; Ibadan, Nigeria, p. 1-133.
Reynolds JM. 2011. An introduction to applied and environmental geophysics. John Wiley & Sons, Ltd, Sussex, England, ISBN 978-0-471-48535-3.
Reynolds JM, Catt LML, Salaün G, Knight P, Cleverly W, Costa L. 2017. Integration of geophysical, geological and

geotechnical data for offshore wind farms – East Anglia one OWF, Southern North Sea, a case history. Offshore Site Investigation Geotechnics 8th International Conference Proceeding, Society for Underwater Technology. 1291–1298(8). doi: 10.3723/OSIG17.1291.

Rogers JD. 2009. Gow, Mohr, Terzaghi, and the origins of the standard penetration test. In: Joint meeting, association of environmental & engineering geologists. Chicago (IL): American Society of Civil Engineers.

Rumpf M, Tronicke J. 2014. Predicting 2D geotechnical parameter fields in near-surface sedimentary environments. J Appl Geophys. 101:95–107. doi: 10.1016/j.jappgeo.2013.12.002.

Sahoo B, Misra D, Daanen RP, Lloyd T, Newby G. 2007. Application of geophysical and spectral methods in non-invasive characterization of porous media: a critical review. 2007 minneapolis, Minnesota, June 17-20, 2007. doi: 10.13031/2013.22990.

Sanders S. 1994. Unanticipated environmental costs in construction contracts: the differing site conditions clause as risk allocation tool. J Nat Resour Environ Law. 10 (1):53–82.

Selvam S, Mukundan M, Alagirisamy S. 2020. Standard penetration test (SPT) pitfalls and improvements. Proceedings of Indian Geotechnical Conference 2020 December 17-19, 2020; Visakhapatnam, India: Andhra University.

Sengupta D, Chen R, Meadows ME. 2018. Building beyond land: an overview of coastal land reclamation in 16 global megacities. Appl Geogr. 90:229–238. doi: 10.1016/j.apgeog.2017.12.015.

Sheng C, Jiao JJ, Liu Y, Luo X. 2022. Impact of major nearshore land reclamation project on offshore groundwater system. Eng Geol. 303:106672. doi: 10.1016/j.enggeo.2022.106672.

Telford WM, Geldart LP, Sheriff RE, Keys DA. 1976. Applied geophysics Vol. xvii, 860. Cambridge, (UK): Cambridge University Press.

Tijani MN. 2023. Geology of Nigeria. In: Faniran A, Jeje LK, Fashae OA Olusola AO, editors. Landscapes and landforms of Nigeria. World geomorphological landscapes. Cham: Springer. doi: 10.1007/978-3-031-17972-3_1.

Vander Velpen BPA. 2004. WinRESIST version 1.0 resistivity depth sounding interpretation software. M. Sc reseach project. ITC, Delft Netherland.

Wagner C. 2020. Best practices in standard penetration testing for liquefaction studies with consideration of uncertainty 41. Missouri University of Science and Technology GE6400 SS20 Practice-Oriented Project.

Ward SH, (ed.). 1990. Geotechnical and environmental geophysics Vol. I-III. Tulsa (OK): SEG, ISBN 978-0931830990.

Woakes M, Ajibade CA, Rahaman MA. 1987. Some metallogenetic features of the Nigerian basement. J Afr Earth Sci. 6(5):655–664. doi: 10.1016/0899-5362(87)90004-2.

Zhang J, Lu C, Werner AD. 2021. Analytical and experimental investigation of the impact of land reclamation on steady-state seawater extent in coastal aquifers. Water Resour Res. 57(6):e2020WR029028. doi: 10.1029/2020WR029028.